Atmos. Chem. Phys. Discuss., 8, 18007–18037, 2008
www.atmos-chem-phys-discuss.net/8/18007/2008/

Atmospheric Chemistry and Physics Discussions

This discussion paper is/has been under review for the journal *Atmospheric Chemistry and Physics (ACP)*. Please refer to the corresponding final paper in *ACP* if available.

A self-adapting and altitude-dependent regularization method for atmospheric profile retrievals

M. Ridolfi[1] **and L. Sgheri**[2]

[1]Dipartimento di Chimica Fisica e Inorganica, Università di Bologna, Bologna, Italy
[2]Istituto per le Applicazioni del Calcolo, Consiglio Nazionale delle Ricerche, Firenze, Italy

Received: 8 July 2008 – Accepted: 27 August 2008 – Published: 10 October 2008

Correspondence to: M. Ridolfi (marco.ridolfi@unibo.it)

Published by Copernicus Publications on behalf of the European Geosciences Union.

Abstract

MIPAS is a Fourier transform spectrometer, operating onboard of the ENVISAT satellite since July 2002.The online retrieval algorithm produces geolocated profiles of temperature and of volume mixing ratios of six key atmospheric constituents: H_2O, O_3, HNO_3, CH_4, N_2O and NO_2. In the validation phase, oscillations beyond the error bars were observed in several profiles, particularly in CH_4 and N_2O.

To tackle this problem, a Tikhonov regularization scheme has been implemented in the retrieval algorithm. The applied regularization is however rather weak in order to preserve the vertical resolution of the profiles.

In this paper we present a self-adapting and altitude-dependent regularization approach that detects whether the analysed observations contain information about small-scale profile features, and determines the strength of the regularization accordingly. The objective of the method is to smooth out artificial oscillations as much as possible, while preserving the fine detail features of the profile when related information is detected in the observations.

The proposed method is checked for self consistency, its performance is tested on MIPAS observations and compared with that of a few scalar and altitude-dependent regularization schemes available in the literature. In all the considered cases the proposed scheme achieves a good performance, thanks to its altitude dependence and to the constrains employed, which are specific of the inversion problem under consideration. The proposed method is generally applicable to iterative Gauss-Newton algorithms for the retrieval of vertical distribution profiles from atmospheric remote sounding measurements.

1 Introduction

MIPAS (Michelson Interferometer for Passive Atmospheric Sounding, Fischer et al. 2008) is a Fourier transform spectrometer operating onboard of ENVISAT, a satellite launched by the European Space Agency (ESA) on 1 March 2002 in a polar orbit. MIPAS measures the atmospheric limb-emission spectrum in the middle infrared (from 685 to 2410 cm^{-1}), a spectral region containing the signatures of the vibrational transitions of many atmospheric constituents. Beyond pressure at the tangent points, the ESA online retrieval algorithm produces geolocated profiles of temperature (T) and of Volume Mixing Ratios (VMR) of six key atmospheric constituents: H_2O, O_3, HNO_3, CH_4, N_2O and NO_2.

The MIPAS measurements from July 2002 to March 2004, consisting of scan patterns of 17 sweeps in the 6–68 km altitude range with 3 km steps in the lower atmosphere, were extensively validated by several research groups (see Atmos. Chem. Phys. 2006 special issue on MIPAS). Oscillations beyond the error bars were observed in several MIPAS profiles, particularly in CH_4 and N_2O VMR (Payan et al., 2007). Starting from January 2005 MIPAS is operated at a reduced spectral resolution with a nominal scan pattern consisting of 27 sweeps in the 6–68 km altitude range with 1.5 km steps in the lower atmosphere. The field of view of the instrument is approximately 3 km in the vertical, so the atmosphere turns out to be oversampled. Since the ESA retrieval grid coincides with the tangent altitudes of the measurements, the finer sampling of the vertical profiles is expected to amplify the unphysical oscillations already present in the measurements acquired until March 2004.

To tackle this problem, a Tikhonov regularization scheme has been implemented in the ESA retrieval algorithm. The choice of the Tikhonov parameter determines the trade-off between the smoothing of the oscillations and the preservation of small-scale features. In the ESA retrieval the adopted choice for the strength of the regularization is rather conservative, to guarantee that small-scale profile features in the altitude domain are preserved (Ceccherini, 2005).

In this paper we present a self-adapting and altitude-dependent regularization approach that detects whether the actual observations contain information about small-scale profile features, and determines the strength of the regularization accordingly. The objective of the method is to smooth out artificial oscillations as much as possible, while preserving the fine detail features of the profile when related information is detected in the observations.

In Sect. 2 we outline the theoretical background of the developed regularization scheme and in Sect. 3 we test the implemented algorithm with synthetic observations. In Sect. 4 we compare the method with other regularization techniques on a single MIPAS limb scan, while in Sect. 5 we extend the comparison to a whole MIPAS orbit. Finally in Sect. 6 we draw conclusions and outline the future developments.

2 Theoretical basis

Ill-conditioning is a common feature of many inverse atmospheric problems. In the case of the retrieval of vertical atmospheric profiles from spectroscopic limb measurements, ill-conditioning produces oscillations in the retrieved profiles beyond the error margins defined by the mapping of the measurement noise into the solution. Tikhonov regularization is often used to improve the conditioning of the inversion. Smoother profiles are obtained by penalizing the oscillating solutions in the inversion formula.

Let $\boldsymbol{y} = \boldsymbol{f}(\boldsymbol{x})$ be the forward problem, where $\boldsymbol{y}$ is the $m-$dimensional vector of the observations with error covariance matrix $\mathbf{S}_\mathrm{y}$, $\boldsymbol{f}$ is the forward model, function of the $n-$dimensional atmospheric state vector $\boldsymbol{x}$. The Tikhonov solution is the state vector $\boldsymbol{x}_\mathrm{t}$ minimising the following cost function:

$$\xi^2 = \|\mathbf{S}_\mathrm{y}^{-\frac{1}{2}}(\boldsymbol{y} - \boldsymbol{f}(\boldsymbol{x}))\|^2 + \lambda\|\mathbf{L}(\boldsymbol{x}_\mathrm{a} - \boldsymbol{x})\|^2 \quad (1)$$

where $\|\cdot\|$ is the ℓ_2 norm, $\boldsymbol{x}_\mathrm{a}$ is an a-priori estimate of the solution, $\mathbf{L}$ is a $l \times n$ matrix operator, usually approximating the $i-th$ order vertical derivative (i=0, 1, 2). Note that normally l=$n-i$. Finally λ is the non-negative scalar Tikhonov parameter driving the strength of the regularization. When i=0, Tikhonov regularization is equivalent to the optimal estimation (OE) method introduced by Rodgers (1976). The first term of the right side of Eq. (1) is referred as χ^2 and represents the cost function minimised in the least–squares approach.

ACPD

8, 18007–18037, 2008

The choice of λ is a crucial step. If the selected λ is too small, a poor regularization will be achieved, whilst if λ is too large, $\mathbf{L}\boldsymbol{x}_t$ will be strongly biased toward $\mathbf{L}\boldsymbol{x}_a$. Many general methods have been proposed for the selection of λ, such as cross validation (Allen, 1974), generalised cross validation (GCV) (Wahba 1977 and Golub et al. 1979), the L-curve method (LC) (Lawson and Hanson 1974 and Hansen 1992) and the discrepancy principle (Morozov, 1993). See e.g. Choi et al. (2007) for a recent paper on the comparison of the various techniques. See also the monographic issue of June 2008 of the Inverse Problems journal.

On the other hand better results may be expected if the operator $\mathbf{L}$ and the value of λ are adapted to the problem under investigation. The following references deal with the inversion of atmospheric state parameters. The LC method has been adopted in Schimpf and Schreier (1997) and more recently in Doicu et al. (2004). A-priori estimates of the degrees of freedom or of the retrieval error have been used by Steck (2002) to get λ. Alternatively Sofieva et al. (2004) tested both the discrepancy principle and vertical resolution requirements for the determination of λ. The error consistency (EC) method proposed by Ceccherini (2005) determines λ analytically by imposing the consistency of the difference between the regularized and the unregularized profiles with the error bars of the regularized profile.

In this paper we propose an altitude-dependent regularization scheme. Though there are more general mathematical formulations we only treat the case of a diagonal $I \times I$ positive semi-definite matrix $\boldsymbol{\Lambda}$. Assuming that $\left.\frac{d^i x}{dz^i}\right|_{z=z_j} \sim (\mathbf{L}\boldsymbol{x})_j$, we may think of $\boldsymbol{\Lambda}_{jj}$ as the regularization strength at altitude z_j. Thus we may speak of a vertical profile of $\boldsymbol{\Lambda}$. Then Eq. (1) becomes:

$$\xi^2 = (\boldsymbol{y} - \boldsymbol{f}(\boldsymbol{x}))^T \mathbf{S}_y^{-1} (\boldsymbol{y} - \boldsymbol{f}(\boldsymbol{x})) + (\boldsymbol{x}_a - \boldsymbol{x})^T \mathbf{L}^T \boldsymbol{\Lambda} \mathbf{L} (\boldsymbol{x}_a - \boldsymbol{x}) \quad (2)$$

Historically, the first idea of a variable regularization, the so-called *localised Tikhonov regularization* has been successfully used in the case of Volterra integral equations (see Lamm (1999) for a good survey). To the best of our knowledge, only few papers deal with variable regularization in other fields. In a recent paper Modarresi and

Golub (2007) show that a vectorial version of the GCV achieves better results than the ordinary scalar version for an image reconstruction problem.

The idea of an altitude-dependent regularization has been used in atmospheric retrievals in Steinwagner and Schwarz (2006), where $\mathbf{\Lambda}=\lambda\mathbf{S}_h$ and $\mathbf{S}_h$ is a diagonal matrix containing the reciprocal of the a-priori estimation of the profile.

In this paper we test altitude-dependent regularization methods determining a profile of $\mathbf{\Lambda}$ as the result of the minimisation of a target function. After the $\mathbf{\Lambda}$-profile is obtained, Eq. (2) is solved via an iterative Gauss-Newton scheme.

Let k be the iteration count, $\mathbf{K}$ be the $m \times n$ Jacobian matrix of $\boldsymbol{f}$ in $\boldsymbol{x}_k$, then the Gauss-Newton iteration for the minimisation of Eq. (2) is:

$$\boldsymbol{x}_{k+1} = \boldsymbol{x}_k + \left(\mathbf{K}^T\mathbf{S}_y^{-1}\mathbf{K} + \mathbf{L}^T\mathbf{\Lambda}\mathbf{L}\right)^{-1}\left[\mathbf{K}^T\mathbf{S}_y^{-1}(\boldsymbol{y} - \boldsymbol{f}(\boldsymbol{x}_k)) + \mathbf{L}^T\mathbf{\Lambda}\mathbf{L}(\boldsymbol{x}_a - \boldsymbol{x}_k)\right] \tag{3}$$

For the determination of $\mathbf{\Lambda}$ we will use the unregularized iterate solution $\boldsymbol{x}_{_{\rm LS}} \equiv \boldsymbol{x}_{k+1}(\mathbf{\Lambda} = \mathbf{0})$. To get $\boldsymbol{x}_{_{\rm LS}}$, the inversion of $\mathbf{K}^T\mathbf{S}_y^{-1}\mathbf{K}$ is required. If this matrix is singular or too much ill–conditioned OE and/or Levenberg–Marquardt terms (see e.g. Rodgers 2000) can be easily included in the presented formulas.

Fix any $\mathbf{\Lambda}$ and let $\boldsymbol{x}_\Lambda$ be the profile minimising Eq. (2). For moderately non-linear problems and a suitable initial guess, $\boldsymbol{x}_k$ converges to $\boldsymbol{x}_\Lambda$. The covariance matrix $\mathbf{S}_\Lambda$ mapping the measurement error $\mathbf{S}_y$ into the solution $\boldsymbol{x}_\Lambda$ is given by:

$$\mathbf{S}_\Lambda = \left(\mathbf{K}^T\mathbf{S}_y^{-1}\mathbf{K} + \mathbf{L}^T\mathbf{\Lambda}\mathbf{L}\right)^{-1}\mathbf{K}^T\mathbf{S}_y^{-1}\mathbf{K}\left(\mathbf{K}^T\mathbf{S}_y^{-1}\mathbf{K} + \mathbf{L}^T\mathbf{\Lambda}\mathbf{L}\right)^{-1}. \tag{4}$$

In the linear approximation, the spatial response function of $\boldsymbol{x}_\Lambda$ is represented (Rodgers, 2000) by the averaging kernel matrix (AK) $\mathbf{A}_\Lambda$ given by:

$$\mathbf{A}_\Lambda = \left(\mathbf{K}^T\mathbf{S}_y^{-1}\mathbf{K} + \mathbf{L}^T\mathbf{\Lambda}\mathbf{L}\right)^{-1}\mathbf{K}^T\mathbf{S}_y^{-1}\mathbf{K}. \tag{5}$$

Vertical resolution is a measure of the dispersion of the signal, usually calculated via the averaging kernel $\mathbf{A}_\Lambda$. Still following Rodgers (2000), there are many practical ways of measuring the vertical resolution, such as the full width at half height of the AK rows:

$$v_i = \frac{\sum_{j=1}^{n} (\mathbf{A}_\Lambda)_{ij} (z_{j-1} - z_{j+1})}{2(\mathbf{A}_\Lambda)_{ii}} \quad (6)$$

where z_j, $j=1,\ldots,n$ are the altitudes, and $z_0=z_1 + (z_1-z_2)$, $z_{n+1}=z_n + (z_n-z_{n-1})$. Throughout this paper, we use a modified version of Eq. (6), with $|\mathbf{A}_\Lambda|_{ij}$ in place of $(\mathbf{A}_\Lambda)_{ij}$ in order to penalize negative lobes of the averaging kernel. When $\mathbf{A}_\Lambda=\mathbf{I}$, Eq. (6) provides anyway the vertical step $\Delta z_i=(z_{i-1}-z_{i+1})/2$ of the retrieval grid. The Backus–Gilbert spread (Rodgers, 2000) is an alternative measure of the vertical resolution. However, in our tests it provided similar results while being more demanding from the computational point of view.

2.1 Altitude-dependent regularization methods

In this paper we compare a new altitude-dependent approach for the determination of $\boldsymbol{\Lambda}$ that we call *variable strength* (VS) with two other altitude-dependent methods.

A) In the VS method $\boldsymbol{\Lambda}$ is determined as the minimiser of the following target function:

$$\psi_{\mathrm{VS}}(\boldsymbol{\Lambda}) = \frac{1}{\overline{\boldsymbol{x}_\Lambda}} \sqrt{\sum_{j=1}^{n} (\mathbf{S}_\Lambda)_{jj} + \sqrt{\left(\chi^2(\boldsymbol{\Lambda}) - \chi^2(\mathbf{0}) - n w_e^2\right)^+}} + \frac{1}{\overline{\boldsymbol{\Delta z}}} \sqrt{\sum_{j=1}^{n} \left[\left(v_j(\boldsymbol{x}_\Lambda) - w_r \Delta z_j\right)^+\right]^2} \quad (7)$$

where the bar over a vector stands for the average of the vector elements, and a superscript $^+$ stands for the positive part of a function. Finally, w_e and w_r are tunable parameters. In other words, we minimise the error of the regularized profile (first term of ψ_{VS}), with penalization terms that are effective when:

(i) the χ^2 of the regularized solution ($\chi^2(\mathbf{\Lambda})$) increases beyond a threshold nw_e^2 with respect to the χ^2 of the unregularized solution (second term of ψ_{VS}), and/or

(ii) at some altitude z_j the vertical resolution of the regularized solution is degraded beyond a factor w_r with respect to Δz_j (third term of ψ_{VS}).

The calculation of ψ_{VS} requires the evaluation of $\chi^2(\mathbf{\Lambda})$. This quantity is known only after the forward model $\boldsymbol{f}(\boldsymbol{x}_\Lambda)$ is calculated. Since this is a very time consuming operation, we use an approximation of $\chi^2(\mathbf{\Lambda})$ in (7). We have:

$$\begin{aligned}\Delta\chi^2 &\equiv \chi^2(\mathbf{\Lambda}) - \chi^2(\mathbf{0}) = \\ &= (\boldsymbol{y} - \boldsymbol{f}(\boldsymbol{x}_{k+1}))^T \mathbf{S}_{\mathrm{y}}^{-1}(\boldsymbol{y} - \boldsymbol{f}(\boldsymbol{x}_{k+1})) - (\boldsymbol{y} - \boldsymbol{f}(\boldsymbol{x}_{\mathrm{LS}}))^T \mathbf{S}_{\mathrm{y}}^{-1}(\boldsymbol{y} - \boldsymbol{f}(\boldsymbol{x}_{\mathrm{LS}})).\end{aligned} \tag{8}$$

It is possible to linearise $\boldsymbol{f}$ about $\boldsymbol{x}_k$, obtaining:

$$\begin{aligned}\boldsymbol{f}(\boldsymbol{x}_{k+1}) &\sim \boldsymbol{f}(\boldsymbol{x}_k) + \mathbf{K}(\boldsymbol{x}_{k+1} - \boldsymbol{x}_k) \\ \boldsymbol{f}(\boldsymbol{x}_{\mathrm{LS}}) &\sim \boldsymbol{f}(\boldsymbol{x}_k) + \mathbf{K}(\boldsymbol{x}_{\mathrm{LS}} - \boldsymbol{x}_k).\end{aligned} \tag{9}$$

Inserting (9) in (8), after some algebraic manipulations we obtain:

$$\Delta\chi^2 \sim (\boldsymbol{x}_{k+1} - \boldsymbol{x}_{\mathrm{LS}})^T \left[-2\mathbf{K}^T \mathbf{S}_{\mathrm{y}}^{-1}(y - \boldsymbol{f}(\boldsymbol{x}_k)) + \mathbf{S}_{\mathrm{x}}^{-1}(\boldsymbol{x}_{k+1} + \boldsymbol{x}_{\mathrm{LS}} - 2\boldsymbol{x}_k)\right] \tag{10}$$

where $\mathbf{S}_{\mathrm{x}}^{-1} \equiv \mathbf{K}^T \mathbf{S}_{\mathrm{y}}^{-1} \mathbf{K}$. When no LM or OE modifications are employed, Eq. (10) may be further simplified. Plugging Eq. (3) with $\mathbf{\Lambda} = \mathbf{0}$ in place of $\boldsymbol{x}_{\mathrm{LS}}$ in (10) we obtain:

$$\Delta\chi^2 \sim (\boldsymbol{x}_{k+1} - \boldsymbol{x}_{\mathrm{LS}})^T \mathbf{S}_{\mathrm{x}}^{-1}(\boldsymbol{x}_{k+1} - \boldsymbol{x}_{\mathrm{LS}}). \tag{11}$$

Expression (11) shows the meaning of the factor w_e in (7): on average the regularized and the unregularized profiles should differ by less than a fraction w_e of the error bar of the unregularized profile. The averaging of residuals at different altitudes involved in the total χ^2 may in principle cause over-regularization if an isolated profile bump is encountered. Therefore we also tested some more restrictive versions of the second term of ψ_{VS}, in which the χ^2 increase is penalized at each individual altitude, similarly to the vertical resolution. The results however did not change significantly. Therefore we preferred to stay with the formulation of Eq. (7) which checks the overall increase of the χ^2, consistently with the actual implementation of the convergence criteria of the retrieval algorithm. The parameters w_e and w_r drive the strength of the regularization. As outlined above, these parameters reflect general requirements on the retrieval and therefore they do not depend on the shape of the actual profile.

B) In the vectorial version of the GCV approach the optimal value of $\mathbf{\Lambda}$ is obtained as the minimiser of the target function ψ_{GCV} defined as in Modarresi and Golub (2007). Within our framework ψ_{GCV} becomes:

$$\psi_{\text{GCV}}(\mathbf{\Lambda}) = \frac{\chi^2(\mathbf{\Lambda})}{\frac{1}{m}\left(m - \text{trace}(\mathbf{A}_{\Lambda})\right)^2}. \tag{12}$$

This expression shows that the GCV method selects a $\mathbf{\Lambda}$-profile with the smallest possible number of degrees of freedom for the retrieval (given by trace($\mathbf{A}_{\Lambda}$)) compatibly with a small $\chi^2(\mathbf{\Lambda})$. In our implementation we calculate $\chi^2(\mathbf{\Lambda}) = \chi^2(\mathbf{0}) + \Delta\chi^2$, with $\Delta\chi^2$ given by Eq. (10) as in the VS method. The vertical resolution of the regularized profile is factored in the GCV method only through the $\chi^2(\mathbf{\Lambda})$. However, the $\chi^2(\mathbf{\Lambda})$ may be not sensitive to vertical resolution, e.g. when attempting the retrieval of a constant vertical profile. In this case the GCV approach produces profiles with dramatically degraded vertical resolution. On the other hand, when $m \gg n$ as in our case, the variation of the denominator in Eq. (12) may be marginal compared with that of the numerator. Therefore, even with a mild dependence of $\chi^2(\mathbf{\Lambda})$ on $\mathbf{\Lambda}$, the regularization produced by the GCV method may be very weak.

C) To overcome the drawbacks of the GCV approach, we also tested a scaled GCV method (SGCV), in which we first find a $\mathbf{\Lambda}$-profile as in the GCV approach, then we multiply it by a scalar factor determined with the VS approach.

ACPD
8, 18007–18037, 2008

2.2 Minimisation of the target function ψ

While the diagonal matrix $\mathbf{\Lambda}$ has always dimension $l \times l$, it is possible to represent the vertical $\mathbf{\Lambda}$-profile with fewer base points. The required $\mathbf{\Lambda}(z_j)$ strengths are then calculated via linear interpolation in altitude between base points. This approach has the advantage of reducing the number of unknowns in the minimisation of the ψ functions (ψ_{VS} and ψ_{GCV} defined in Sect. 2.1), thus shortening the calculation time. The number of points used to represent the $\mathbf{\Lambda}$-profile however should be sufficient to allow an adequate altitude variability of the regularization strength. On the other hand it is useless to employ more than $l = n-i$ points for the representation of the $\mathbf{\Lambda}$-profile.

Due to the large amount of local minima, analytical methods like conjugate gradients do not perform well when applied to the minimisation of ψ. We found better results using the simulated annealing method (see e.g. Press et al., 1992, Sect. 10.9).

For the efficiency of the algorithm, we allow negative elements of the $\mathbf{\Lambda}$-profile and take the absolute values, instead of bounding them to be positive. Fine tuning of the $\mathbf{\Lambda}$-profile is not rewarded by the inversion procedure, therefore the minimisation can be stopped as soon as the location of the minimum is approached. In this way it is possible to limit the computational overhead required by the minimisation. The $\mathbf{\Lambda}$-profile corresponding to the minimum of ψ depends on the vertical shape of the actual profile $\boldsymbol{x}_{\text{LS}}$ which, in turn, exhibits a large variability in the atmosphere. The lack of a preferred shape for the $\mathbf{\Lambda}$-profile makes it impossible to predict an a–priori *annealing temperature* for which the process should be stopped. To avoid useless calculations, the process should also be stopped when repeatedly failing to reduce significantly the target function.

We tried several implementations of the simulated annealing method, and we found the best results with the routine SA of Goffe (1994). The settings of this routine were optimised according to the guidelines mentioned above. In this way we achieved a much faster convergence compared to the standard settings suggested by the authors.

3 Results of simulated retrievals

We implemented the VS regularization method in the Optimised Retrieval Model (ORM, see Ridolfi et al. 2000; Raspollini et al. 2006) that is used by ESA for near real–time inversion of MIPAS data (Fischer et al., 2008). For comparison purposes, in the same code we also implemented the GCV and SGCV methods with a selectable switch. All of these methods can be applied either after each Gauss–Newton iteration or as a final step after the convergence of the inversion. However, in general we found that applying regularization after each iteration leads to heavier calculations and a slower convergence rate, with no benefits on the results (in agreement with findings reported in Ceccherini et al. 2007). As a consequence in all the test cases presented in this paper we applied the regularization only after reaching the convergence of the inversion. In all the tests presented we selected the regularization operator $\mathbf{L}=\mathbf{L}_2$, the second derivative operator, with an exception for the EC method which is implemented in the ORM with $\mathbf{L}=\mathbf{L}_1$. The choice $\mathbf{L}=\mathbf{L}_2$ produces slightly better results when the profile varies almost linearly with altitude. The regularization schemes take into account the LM approach employed by the ORM, as outlined in Sect. 2.

First we tested the self–consistency of the VS method and its capability to detect possible sharp profile features measured by the instrument. For this purpose we carried out a test O_3 retrieval starting from synthetic observations. These observations were generated by the forward model included in the ORM, using a climatological mean *reference* atmosphere (Remedios et al., 2007) with the O_3 profile modified with a sharp bump in the 18–24 km altitude range. This modification reflects the double–peak feature sometimes observed in the real O_3 profiles for instance in pre–hole conditions (see Nemuc and Dezafra 2005). Instrument features such as field of view, vertical scan pattern and spectral line–shape were adjusted to the MIPAS configuration adopted for the *nominal reduced resolution* measurements acquired from January 2005 onward (Dudhia, 2008). Spectral measurement noise was added to synthetic observations. For altitudes ≤40 km the noise was chosen consistent with MIPAS specifications; for altitudes >40 km the noise was multiplied by a factor 20 in order to obtain amplified oscillations in the unregularized retrieved profile. The VS regularization was applied after the convergence of the unregularized (LS) solution, using a discrete second derivative operator $\mathbf{L}_2$, and parameters $(w_e, w_r)=(1,5)$. The altitude grid of the retrieved profiles consisted of 27 points, coinciding with the tangent points of the limb measurements, while the $\boldsymbol{\Lambda}$-profile consisted of 27−2=25 points. In this particular test case we disabled the LM modification in the ORM.

Figure 1 shows the results of the test. In panel (a) we show the reference profile (solid grey), the initial guess profile (dashed black), the unregularized LS solution (dotted red) and the regularized VS solution (solid blue). The initial guess profile was obtained by multiplying the climatological profile by a factor of 1.3 and with no bump modification. The VS method was able to distinguish between the oscillations of the LS solution due to lack of stability (mainly in the 40–70 km height range, where the error has been artificially amplified) and the real bump present in the reference profile. In the 40–70 km range the oscillations were smoothed out thanks to the large error bars of the LS solution. On the other hand the real bump was retained since the relatively small error bars in this altitude region prevented a strong smoothing. As required by the VS method, on average the VS profile is consistent with the LS profile within a fraction w_e=1 of the LS error bars. This result is illustrated in panel (b) of Fig. 1 which shows the percentage retrieval errors of the LS (dotted red) and VS (dashed blue) solutions (obtained from Eq. 4) and the actual percentage difference between the VS and the reference profiles (solid blue), i.e. the actual error. We note that this difference is mostly consistent with the error of the VS solution. Only below 18 km the regularization introduces a noticeable smoothing error, which is not included in Eq. (4). This error is however consistent with the LS error bounds and is quite small in absolute value (<0.1 ppmv), the profile itself being very close to zero in this altitude range. Panel (c) shows the LS (solid red) and VS (solid blue) vertical resolutions. The LS vertical resolution, as mentioned in Sect. 2, coincides with the vertical limb scanning step of the measurements. The dashed red line shows the maximum allowed vertical resolution for the VS solution, i.e. w_r=5 times the LS vertical resolution. While this upper bound is never violated, we note that in the 20–37 km range this bound is not even approached. This is due to the simultaneous occurrence of small error bars of the LS solution and the changing slope of the reference profile. This combination prevents a stronger VS regularization by triggering the χ^2 penalization term in the ψ_{VS} target function. Panel (d) shows the obtained **Λ**-profile for the VS solution. Note that small values of **Λ** are obtained whenever the above combination occurs.

Figure 2 shows the rows of the AK of the regularized profile. The number of degrees of freedom obtained for the VS profile (the trace of the averaging kernel) was 14.7.

The AK plotted in Fig. 2 is calculated with Eq. (5), thus assuming that the **Λ**-profile derived with the VS method does not depend on the actual VMR profile encountered in the atmosphere. Therefore, the AK of Fig. 2 represents only *locally* (i.e. for the current **Λ**) the spatial response function of the measuring system. We point out that the large width of the AK rows for altitudes >40 km is due to the strong regularization triggered by the artificially amplified noise in the synthetic observations.

4 Results of retrievals from a single MIPAS limb scan

In this section we present the results of retrievals based on MIPAS measurements related to a single limb scan. For this analysis we selected scan number 060 of ENVISAT orbit 15 451 from 12th February 2005. The approximate average latitude of the tangent points is 82° South. This scan shows low stratospheric temperatures, hence a reduced S/N ratio that triggers oscillations in the unregularized retrieval. Moreover, it includes limb views with tangent altitudes penetrating the cloud-free upper troposphere.

4.1 Selection of VS parameters

The choice of the parameters driving the strength of the regularization is often a critical step when they have to be determined by the user on the basis of a tuning procedure.

ACPD
8, 18007–18037, 2008

In fact the tuning is necessarily based on some assumed profile and therefore the results may not be optimal when there is a substantial difference between the actual and the assumed profile.

In the case of the VS method, the strength of the regularization (i.e. the magnitude of the **Λ**-profile) is indirectly driven by the w_e and w_r coefficients. In principle w_e and w_r may be chosen arbitrarily and independently from each other. However, there is a positive correlation between allowed χ^2 increase and vertical resolution degradation, therefore not all the couples (w_e, w_r) are equally meaningful. For instance, if a small w_r is imposed, the difference between the regularized and unregularized profiles will be small, and therefore the increase of χ^2 will also be small, so that a large value of w_e would make ineffective the related constraint.

This concept is illustrated in Fig. 3, which is a colour map of the logarithm of the minimum of the target function ψ_{VS} of Eq. (7) as a function of w_e and w_r for CH_4 retrieval. From this map we see that well chosen couples (w_e, w_r) are those for which variations of the target function minimum occur for small variations of any of the two parameters. This situation occurs in Fig. 3 around the diagonal from bottom-left to top-right. Analogous maps for the other MIPAS retrieval targets show the same behaviour for roughly the same values of (w_e, w_r).

From the previous considerations one may argue that a single parameter w_e or w_r could be sufficient to control both the vertical resolution degradation and the χ^2 increase. While this is true for most MIPAS retrieval targets, the double constraint in ψ_{VS} ensures, with very little overhead added, a good behaviour even in some *pathological* conditions. These include, for instance, the case of an almost linear profile versus altitude, or the case of very large relative error bars such as in the case of NO_2 retrievals above 60 km. In both cases a single limitation on the χ^2 increase would lead to profiles with a dramatically degraded vertical resolution. In the NO_2 case, this also produces a regularized profile with a physically unacceptable shape. On the other hand a single constraint on the vertical resolution leads to the loss of detailed features of the profile also in the case of relatively small error bars, such as in the double-peaked O_3 profile

ACPD

8, 18007–18037, 2008

retrieval considered in Sect. 3.

Figure 4 reports the obtained CH_4 profiles for some (w_e, w_r) couples. The related χ^2 increase with respect to the LS method is reported in the legend. We see that the couple $(w_e, w_r)=(1, 5)$ permits to achieve a strong enough regularization with a marginal increase (0.56%) of the χ^2. Therefore we will use this couple for the tests reported hereafter in this section.

4.2 Comparison of altitude-dependent regularizations

In this subsection we briefly compare the VS method with the other altitude-dependent techniques (GCV and SGCV) introduced in Sect. 2. The purpose of this comparison is twofold. On one side we show that the $\mathbf{\Lambda}$-profiles obtained with the VS method have some correlation with those obtained with other more general methods such as the vectorial version of GCV. On the other hand we also show that the VS method achieves better results by implementing constraints specific to the inversion problem under consideration.

Figure 5 illustrates the results of the comparison for the retrieval of CH_4. The obtained $\mathbf{\Lambda}$-profiles, reported in panel (d), show similar shapes as a function of altitude. As shown in panel (c) the GCV method produces a dramatic degradation of the vertical resolution in the 25–40 km altitude range. To restore the vertical resolution constraint of the VS method, the scaling factor of SGCV is less than 0.001. As a consequence the regularization achieved by the SGCV method is very weak, as confirmed by panel (a) and (b), reporting profiles and errors respectively. Despite the generally large degradation in vertical resolution, the GCV method is not able to smooth out the feature of the LS profile in the 10–15 km range. On the other hand this objective is achieved by the VS method with only the marginal χ^2 increase mentioned above (0.56%).

4.3 Comparison of VS method with self adapting scalar regularizations

In this subsection we compare the VS method with the LC and EC scalar regularization methods already introduced in Sect. 2, using the retrievals of CH_4, O_3 and H_2O as test cases. The results are illustrated in Figs. 6, 7 and 8 respectively.

We see that with the rather strong choice of $(w_e, w_r)=(1, 5)$ the VS method is able to smooth out quite large oscillations, such as those in the H_2O profile above the tropopause. Due to the large variability of the water profile across the retrieval altitude range, these oscillations could not be smoothed by any of the scalar methods considered.

On the other hand, in the ozone retrieval small error bars suggest that the feature in the 20–26 km range may be real. In this case, both the EC and VS methods are able to preserve this feature, while the LC method smooths it out badly.

These results indicate that the VS method, due to its adaptive capability, is able to achieve a strong regularization while preserving small-scale profile features when the LS profile errors are small compared with the amplitude of the feature itself.

5 Results of retrievals from a full MIPAS orbit

In this section we analyse the performance of the VS method based on MIPAS measurements related to the full ENVISAT orbit 15451. The orbit consists of 79 nominal scans (Dudhia, 2008). Several measurements related to scan 4 are however corrupted, therefore the retrieval is performed only on 78 scans. Visual inspection of individual profiles from such a large sample is unpractical, so we introduce some quantifiers to characterise the average performance of the retrieval.

The first quantifier we consider is $\bar{\chi}^2_R$, which is the arithmetic mean (on the orbit) of the normalised chi-square χ^2_R (see Bevington and Robinson 2003) related to individual profiles.

ACPD

8, 18007–18037, 2008

A self-adapting regularization method

M. Ridolfi and L. Sgheri

To measure the smoothness of a profile we introduce an oscillation quantifier Ω_2 that, for a single profile $x_i = x(z_i)$, $i = 1, \ldots, n$ is defined as

$$\Omega_2 = 100 \cdot \sqrt{\frac{1}{n-2} \sum_{i=2}^{n-1} \left[x_i - x_{i-1} - \frac{x_{i+1} - x_{i-1}}{z_{i+1} - z_{i-1}} (z_i - z_{i-1}) \right]^2}. \quad (13)$$

The quantity Ω_2 represents the root mean square distance between each profile point x_i and the linear interpolation at z_i from the two adjacent points x_{i-1} and x_{i+1}. The factor 100 is introduced for better readability of the actual numbers. Note that Ω_2=0 if and only if the profile is a line. Moreover, when the z_i are equispaced, Ω_2 is proportional to the ℓ_2 norm of the discrete second derivative of the profile. We then take the arithmetic mean $\bar{\Omega}_2$ (on the orbit) of the Ω_2 related to individual profiles.

We compare the VS method with three different (w_e, w_r) couples with the LS (no regularization) and the EC methods. For each of the VS tests, $\boldsymbol{\Lambda}$-profiles with 9 base points have been used. We found that the LC method poses some problems when there is no user supervision of the individual retrievals. In fact it turns out that the L-curve is not always really *L-shaped*. In these cases the values of the λ parameter obtained for the maximum of curvature may be meaningless.

Table 1 shows the results of the test. The first row contains the list of methods, the parameters (w_e, w_r) used in the VS method are shown in parenthesis. For each retrieval target and each method considered we report the values of $\bar{\chi}_R^2$ and $\bar{\Omega}_2$. The last row of the table contains the percentage variation of $\bar{\chi}^2$ and $\bar{\Omega}_2$ with respect to the LS method, averaged over the retrieval targets.

We note that the weakest VS regularization considered $(w_e, w_r) = (0.6, 3)$ already provides on average both a smaller $\bar{\chi}_R^2$ increase and a larger $\bar{\Omega}_2$ reduction with respect to the EC scalar method. A further reduction of the $\bar{\Omega}_2$ is achieved by the VS method with $(w_e, w_r) = (1, 5)$ with $\bar{\chi}_R^2$ values close to those of EC. The VS method with $(w_e, w_r) = (2, 8)$ achieves a further reduction of the $\bar{\Omega}_2$ at the expenses of a quite large $\bar{\chi}_R^2$ increase.

ACPD

8, 18007–18037, 2008

The advantages of the VS method are particularly noticeable in the case of the H_2O, CH_4 and N_2O target species. The H_2O profile probably gets a particular benefit from different strengths of regularization that are applied above and below the tropopause. Above the tropopause a strong regularization can be applied since the profile is almost linear with altitude. Below the tropopause only a weak regularization can be applied since the profile deviates significantly from linearity. In the case of CH_4 and N_2O, there are quite large altitude intervals where the profiles behave almost linearly so that the VS method can apply a strong regularization without significant $\bar{\chi}_R^2$ increase. We note that these are the two MIPAS species for which unphysical oscillations were reported in the validation phase (see Payan et al. 2007).

The computational overhead introduced by the VS method depends on the number of base points used for the $\mathbf{\Lambda}$-profile, and on how often the $\mathbf{\Lambda}$-profile is updated (i.e. how often the minimisation of ψ_{VS} is carried out). Within our setup (9 base points and $\mathbf{\Lambda}$-profile updated every scan) the overall runtime increase is less than 20% with respect to the LS method. This is a quite encouraging result, considering that in operational retrievals fewer base points might be sufficient to achieve a good regularization and also that the $\mathbf{\Lambda}$-profile could be updated only when strictly necessary. Update of $\mathbf{\Lambda}$ is in fact necessary only when the actual unregularized VMR profile encountered in the atmosphere is significantly different (i.e. beyond a few error bars) from the VMR profile used for the last calculation of $\mathbf{\Lambda}$.

6 Conclusions

In this work we introduce a new self-adapting method (VS) for determination of the altitude dependent strength of Tikhonov regularization. The method can be applied to the retrieval of vertical distribution profiles from observations sounding the atmosphere either at the limb or vertically.

We first prove the self-consistency of the implemented algorithm on the basis of synthetic limb-scanning observations. Secondly we test the method using real MIPAS observations. We compare the performance of the method with that of some scalar (LC and EC) and altitude-dependent (GCV, SGCV) regularization schemes available in the literature. In all the tested cases the VS method achieves a better performance than the other methods, thanks to its altitude dependence and to the constrains employed, which are specific of the inversion problem under consideration.

The self-adaptability of the VS method permits to obtain a sufficiently strong regularization and, at the same time, the risk of over-smoothing sharp profile features is avoided when related information is present in the analysed observations.

Future developments will tackle the optimization of the algorithm for operational MIPAS data analysis and its extention to 2-D retrieval schemes.

The proposed method can be implemented in any Gauss-Newton-type algorithm for the retrieval of vertical distribution profiles. Currently the VS algorithm is coded in a standard FORTRAN routine both in a stand-alone version and in a version interfaced with the ORM code. The routine can be easily interfaced with any existing inversion software. The authors will be happy to freely supply the VS routine to scientists that would like to test the algorithm in their inversion codes, for no-profit purposes.

Acknowledgements. The authors would like to thank Bruno Carli, Massimo Carlotti and Simone Ceccherini for fruitful discussions. We also thank the IFAC-CNR institute in Firenze for making available computing and technical facilities through associate contract to M.R., in the frame of the research activity TA.P06.002.

References

Allen, M: The relationship between variable selection and data augmentation and a method for prediction, Technometrics, 16, 125–127, 1974. 18011

Bevington, P. R. and Robinson, D. K.: Data Reduction and Error Analysis for the Physical Sciences, 3rd ed. McGraw–Hill, New York, 384 pp., 2003. 18022

Ceccherini, S.: Analytical determination of the regularization parameter in the retrieval of atmospheric vertical profiles, Opt. Lett., 30(19), 2554–2556, 2005. 18009, 18011

Ceccherini, S., Belotti, C., Carli, B., Raspollini, P., and Ridolfi, M.: Technical Note: Regularization performances with the error consistency methos in the case of retrieved atmospheric profiles, Atmos. Chem. Phys., 7, 1435–1440, 2007, http://www.atmos-chem-phys.net/7/1435/2007/. 18017

Choi, H. G., Thite, A. N., and Thompson, D. J.: Comparison of methods for parameter selection in Tikhonov regularization with application to inverse force determination, J. Sound Vib., 304, 894–917, 2007. 18011

Doicu, A., Schreier, F., and Hess, M.: Iterative regularization methods for atmospheric remote sensing, J. Quant. Spectrosc. Ra., 83, 47–61, 2004. 18011

Dudhia, A.: MIPAS-related section of the web-site of the Oxford University: www.atm.ox.ac.uk/group/mipas, last access: 1 July 2008, 2008. 18017, 18022

Fischer, H., Birk, M., Blom, C., Carli, B., Carlotti, M. , von Clarmann, T., Delbouille, L., Dudhia, A., Ehhalt, D., Endemann, M., Flaud, J.-M., Gessner, R. , Kleinert, A., Koopmann, R., Langen, J., López-Puertas, M., Mosner, P., Nett, H., Oelhaf, H., Perron, G., Remedios, J., Ridolfi, M., Stiller, G., and Zander, R.: MIPAS: an instrument for atmospheric and climate research, Atmos. Chem. Phys., 8, 2151–2188, 2008, http://www.atmos-chem-phys.net/8/2151/2008/. 18008, 18017

Goffe, W. L., Ferrier, G. D., and Rogers, J.: Global Optimization of Statistical Functions with Simulated Annealing, J. Econometrics, 60, 65–100, 1994. 18016

Golub, G. H., Heath, M., and Wahba, G.: Generalized cross-validation as a method for choosing a good ridge parameter, Technometrics, 21 (2), 215–223, 1979. 18011

Hansen, P. C.: Analysis of discrete ill-posed problems by means of the L-curve, SIAM Rev., 34, 561–580, 1992. 18011

Lamm, P. K.: Some Recent Developments and Open Problems in Solution Methods for Mathematical Inverse Problems, Department of Mathematics, Michigan state University, USA, 23 pp., 1999. 18011

Lawson, C. L. and Hanson, R. J.: Solving Least Squares Problems, Prentice-Hall, Englewood Cliffs, 340 pp., 1974. 18011

Modarresi, K. and Golub, G. H.: Using Multiple Generalized Cross-Validation as a Method for Varying Smoothing Effects, CSC2007, The SIAM Workshop on Combinatorial Scientific Computing, San Francisco, 1–2, 2007. 18011, 18015

Morozov, V. A.: Regularization methods for ill-posed problems, CRC Press, Boca Raton, 272 pp., 1993. 18011

ACPD

8, 18007–18037, 2008

Nemuc, A. V. and Dezafra, R. L.: Ground based measurements of stratoshperic ozone in Antarctica, Romanian Reports in Physics, 57(3), 445–452, 2005. 18017

Payan, S., Camy-Peyret, C., Oelhaf, H., Wetzel, G., Maucher, G., Keim, C., Pirre, M., Huret, N., Engel, A., Volk, M. C., Kuellmann, H., Kuttippurath, J., Cortesi, U., Bianchini, G., Mencaraglia, F., Raspollini, P., Redaelli, G., Vigouroux, C., De Mazière, M., Mikuteit, S., Blumenstock, T., Velazco, V., Notholt, J., Mahieu, M., Duchatelet, P., Smale, D., Wood, S., Jones, N., Piccolo, C., Payne, V., Bracher, A., Glatthor, N., Stiller, G., Grunow, K., Jeseck, P., Te, Y., Pfeilsticker, K., and Butz, A.: Validation and data characteristics of methane and nitrous oxide profiles observed by MIPAS and processed with Version 4.61 algorithm, Atmos. Chem. Phys. Discuss., 7, 18 043–18 111, 2007, http://www.atmos-chem-phys-discuss.net/7/18043/2007/. 18009, 18024

Press, W. H., Teukolsky, S. A., Vetterling, W. T., and Flannery, B. P.: Numerical Recipes in C: The Art of Scientific Computing, 2nd ed. Cambridge Univ. Press, Cambridge, 994 pp., 1992. 18016

Raspollini, P., Belotti, C., Burgess, A., Carli, B., Carlotti, M., Ceccherini, S., Dinelli, B. M., Dudhia, A., Flaud, J.-M, Funke, B., Hoepfner, M., López-Puertas, M., Payne, V., Piccolo, C., Remedios, J. J., Ridolfi, M., and Spang, R.: MIPAS Level 2 operational analysis, Atmos. Chem. Phys., 6, 5605–5630, 2006, http://www.atmos-chem-phys.net/6/5605/2006/. 18017

Remedios, J. J., Leigh, R. J., Waterfall, A. M., Moore, D. P., Sembhi, H.,Parkes, I., Greenhough, J., Chipperfield, M. P., and Hauglustaine, D.: MIPAS reference atmospheres and comparisons to V4.61/V4.62 MIPAS level 2 geophysical data sets, Atmos. Chem. Phys. Discuss., 7, 9973–10 017, 2007. 18017

Ridolfi, M., Carli, B., Carlotti, M., von Clarmann, T., Dinelli, B. M., Dudhia, A., Flaud, J.-M., Hoepfner, M., Morris, P. E., Raspollini, P., Stiller, G., and Wells, R. J.: Optimized forward model and retrieval scheme for MIPAS near-real-time data processing, Appl. Optics, 39(8), 1323–1340, 2000. 18017

Rodgers, C. D.: Retrieval of atmospheric temperature and composition from remote measurements of thermal radiation, Rev. Geophys. Space Phys., 14, 609–624, 1976. 18010

Rodgers, C. D.: Inverse Methods for Atmospheric Sounding: Theory and Practice, Vol. 2 of Series on Atmospheric, Oceanic Planet. Phys., World Scientific, Singapore, 238 pp., 2000. 18012, 18013

Schimpf, B. and Schreier, F.: Robust and efficient inversion of vertical sounding atmospheric high–resolution spectra by means of regularization, J. Geophys. Res., 102(D13), 16 037–

16 055, 1997. 18011
Sofieva, V. F., Tamminen, J., Haario, H., Kyröla, E., and Lethinen, M.: Ozone profile smoothness as a priori information in the inversion of limb measurements, Ann. Geophys., 22, 3411–3420, 2002, http://www.ann-geophys.net/22/3411/2002/. 18011
Steck, T.: Methods for determining regularization for atmospheric retrieval problems, Appl. Optics, 41(9), 1788–1797, 2002. 18011
Steinwagner, J. and Schwarz, G.: Shape-dependent regularization for the retrieval of atmospheric state parameter profiles, Appl. Optics, 45(5), 1000–1009, 2006. 18012
Wahba, G.: Practical approximate solutions to linear operator equations when the data are noisy, SIAM J. Numer. Anal., 14, 651–667, 1977. 18011

ACPD
8, 18007–18037, 2008

A self-adapting regularization method

M. Ridolfi and L. Sgheri

Table 1. Results from orbit 15451.

		LS	EC	VS(0.6,3)	VS(1,5)	VS(2,8)
T	$\bar{\chi}_R^2$	1.848	1.861	1.861	1.878	1.999
	$\bar{\Omega}_2$	383.590	310.534	283.719	251.254	190.034
H_2O	$\bar{\chi}_R^2$	1.261	1.267	1.261	1.268	1.310
	$\bar{\Omega}_2$	449.590	365.930	289.166	229.185	166.063
O_3	$\bar{\chi}_R^2$	2.575	2.586	2.579	2.583	2.644
	$\bar{\Omega}_2$	41.782	31.227	32.677	29.145	24.775
HNO_3	$\bar{\chi}_R^2$	1.223	1.226	1.219	1.222	1.251
	$\bar{\Omega}_2$	0.085	0.064	0.065	0.061	0.048
CH_4	$\bar{\chi}_R^2$	2.075	2.098	2.088	2.102	2.147
	$\bar{\Omega}_2$	32.754	19.764	15.941	11.539	3.660
N_2O	$\bar{\chi}_R^2$	2.117	2.121	2.116	2.114	2.166
	$\bar{\Omega}_2$	2.900	1.855	1.268	0.806	0.478
NO_2	$\bar{\chi}_R^2$	1.414	1.423	1.422	1.425	1.418
	$\bar{\Omega}_2$	0.463	0.208	0.207	0.145	0.080
Avg.	$\Delta\bar{\chi}_R^2$(%)		+0.533	+0.230	+0.613	+3.301
wrt LS	$\Delta\bar{\Omega}_2$(%)		−31.247	−38.626	−49.694	−64.767

ACPD

8, 18007–18037, 2008

A self-adapting regularization method

M. Ridolfi and L. Sgheri

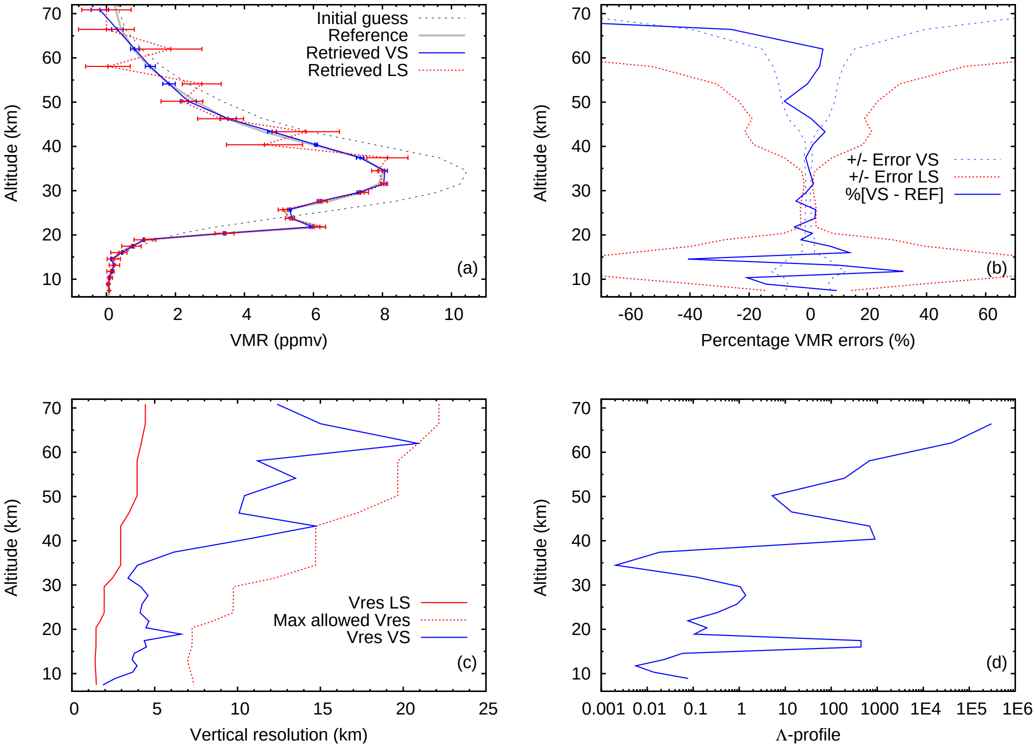

Fig. 1. Simulated O_3 retrieval with an artificial bump from 18 to 24 km added: **(a)** Reference, initial guess and retrieved profiles; **(b)** estimated retrieval errors and actual difference between retrieved and reference profiles; **(c)** vertical resolution; **(d)** **Λ**-profile.

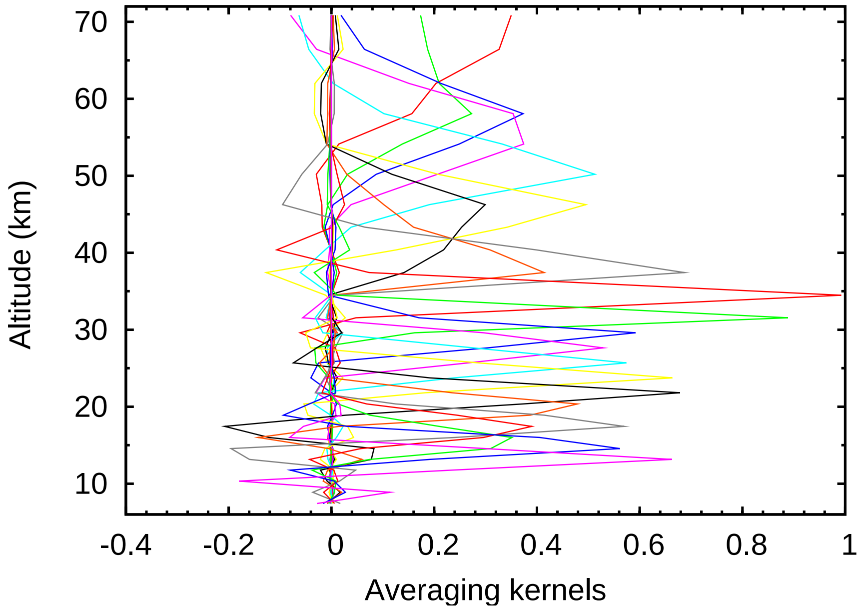

Fig. 2. Simulated O_3 retrieval with an artificial bump from 18 to 24 km added: Averaging kernel rows.

ACPD
8, 18007–18037, 2008

A self-adapting regularization method

M. Ridolfi and L. Sgheri

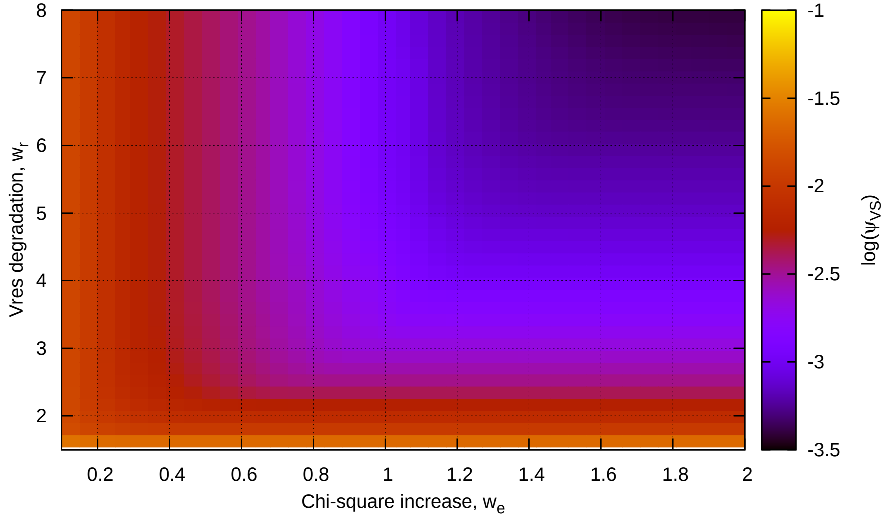

Fig. 3. Map of the logarithm of the minimum of $\psi_{VS}(\mathbf{\Lambda})$ as a function of w_e and w_r for CH_4 retrieval.

ACPD
8, 18007–18037, 2008

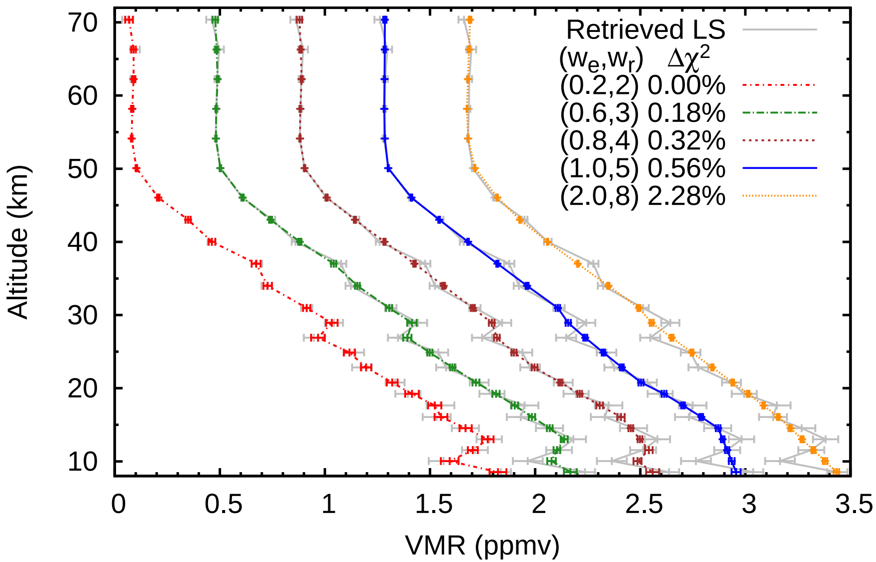

Fig. 4. CH_4 profiles retrieved with the VS method for various (w_e, w_r) couples. Profiles are horizontally shifted by 0.4 ppmv each for a clearer representation. Legend includes percentage χ^2 increase with respect to the LS method.

ACPD

8, 18007–18037, 2008

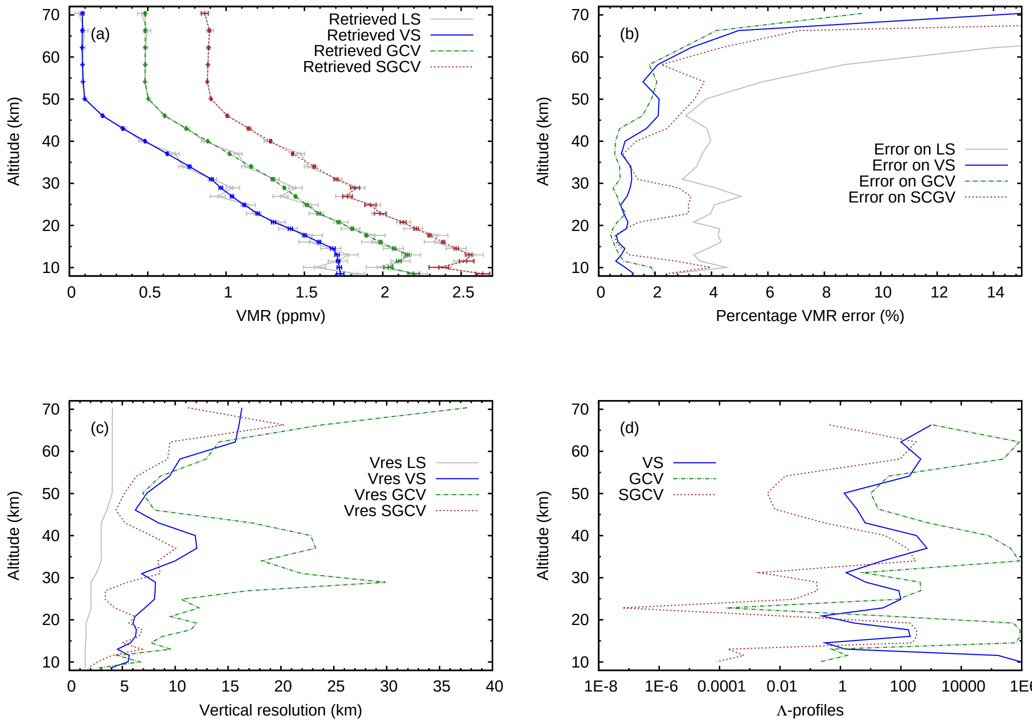

Fig. 5. Retrieval of CH_4 from single scan MIPAS measurements: LS (reference, no regularization), VS, GCV and SGCV regularization techniques. Profiles are horizontally shifted by 0.4 ppmv each for a clearer representation. **(a)** Retrieved profiles; **(b)** estimated retrieval errors; **(c)** vertical resolutions; **(d)** **Λ**-profiles.

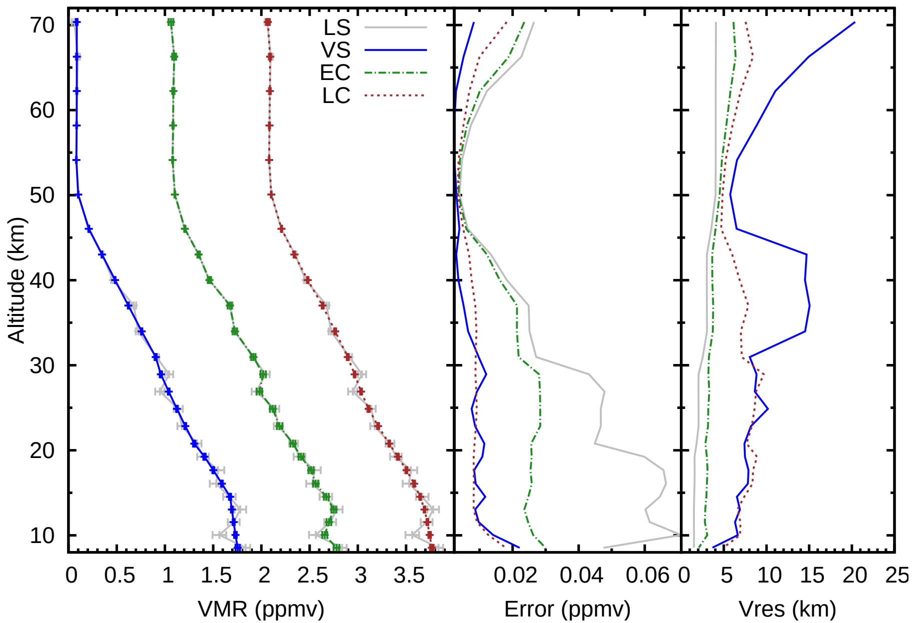

Fig. 6. CH_4 retrieval with VS, EC and LC regularization methods. Profiles (left), errors (centre) and vertical resolution (right). VMR profiles are horizontally shifted for a clearer representation.

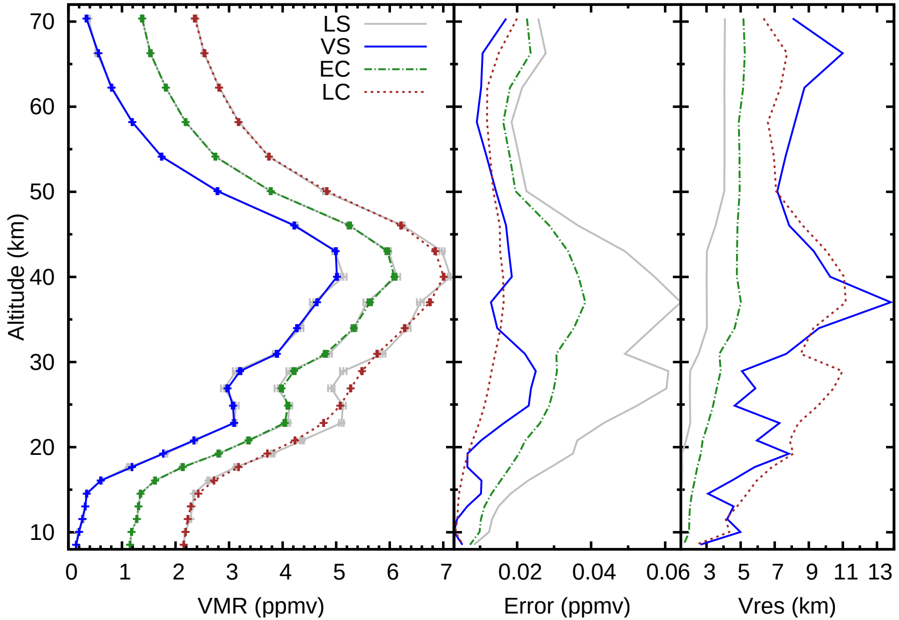

Fig. 7. O_3 retrieval with VS, EC and LC regularization methods. Profiles (left), errors (centre) and vertical resolution (right). VMR profiles are horizontally shifted for a clearer representation.

ACPD
8, 18007–18037, 2008

Title Page
Abstract
Introduction
Conclusions
References
Tables
Figures
◀◀
▶▶
◀
▶
Back
Close
Full Screen / Esc
Printer-friendly Version
Interactive Discussion

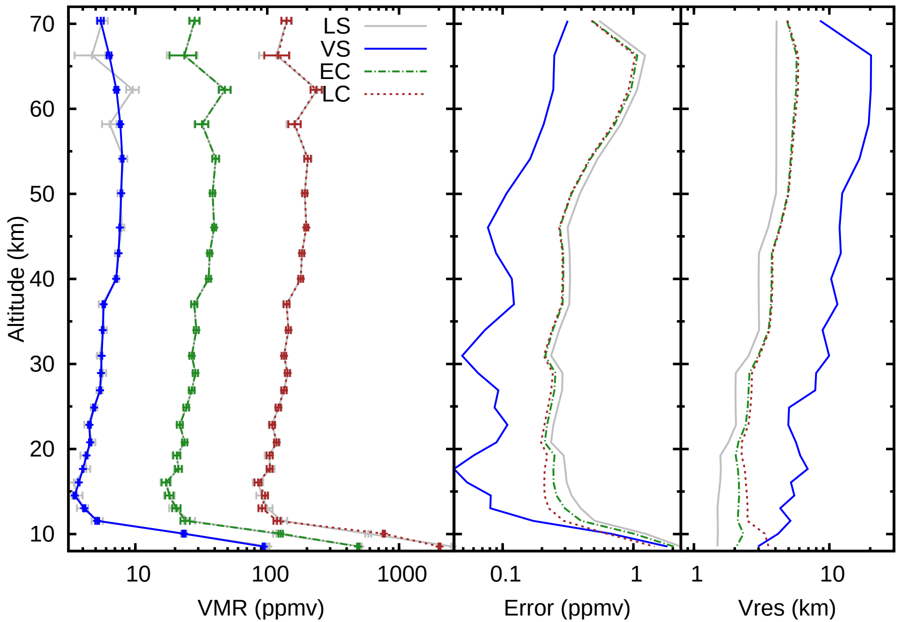

Fig. 8. H_2O retrieval with VS, EC and LC regularization methods. Log-scale plot of profiles (left), errors (centre) and vertical resolution (right). VMR profiles are horizontally scaled for a clearer representation.